Mathematical model of the dynamic behavior of modern railway rolling stock on a curved track section

Andrii Kuzyshyn[1], Vitalii Kovalchuk[2], Andriy Pentsak[3]
[1, 2]Department of Railway Transport, Lviv Polytechnic National University, Lviv, Ukraine
[1]Railway Transport Research Laboratory, Lviv Scientific Research Institute of Forensic Expertise, Lviv, Ukraine
[3]Department of Building Production Lviv Polytechnic National University, Lviv, Ukraine
[1]Corresponding author
E-mail: [1]*andrii.y.kuzyshyn@lpnu.ua*, [2]*vitalii.v.kovalchuk@lpnu.ua*, [3]*andrii.y.pentsak@lpnu.ua*

Received 29 March 2026; accepted 8 October 2026; published online 24 November 2026
DOI https://doi.org/10.21595/mme.2026.26470

Check for updates

Copyright © 2026 Andrii Kuzyshyn, et al. This is an open access article distributed under the Creative Commons Attribution License, which permits unrestricted use, distribution, and reproduction in any medium, provided the original work is properly cited.

Abstract. The object of the study is the safety factor against wheel derailment of the EKr-1 "Tarpan" electric train equipped with a pneumatic suspension system when operating on a curved track section. A spatial mathematical model of the dynamic behavior of rolling stock has been developed, taking into account the specific features of the mechanical linkages in its structure, as well as the conditions of wheel-rail interaction on curved sections of railway track. An analytical description of the functions of lateral rail deviation (horizontal irregularities) in curved track sections has been carried out. Three sections of the curve are considered: the entry transition curve, the circular curve, and the exit transition curve, with account taken of outer rail superelevation and track gauge widening in curves. Regularities in the variation of frame force and safety factors against wheel derailment as functions of curve radius at different speeds have been obtained. It is shown that an increase in curve radius leads to a decrease in frame force and an increase in the safety factor against wheel derailment. It has been established that, based on the safety factor against wheel derailment, the permissible speeds are as follows: for a curve radius of 300 m-80 km/h; 500 m-90 km/h; 800 m-100 km/h; 1000 m-120 km/h; 2000 m-150 km/h; and 3000÷4000 m-160 km/h. It is demonstrated that on curved sections of railway track, the full realization of high-speed operation is not feasible.

Keywords: EKr-1 "Tarpan" electric train, curved railway track section, frame force, safety factor against wheel derailment, mathematical model, curve radius, permissible speed.

1. Introduction

The relevance of using modern rolling stock is driven by the need to increase operating speeds, which contributes to enhancing the line capacity and carrying capacity of railway networks. Before commissioning modern railway rolling stock-already at the design stage and during acceptance tests-its dynamic performance characteristics in interaction with the track are evaluated [1]. One example of modern Ukrainian-built rolling stock is the interregional high-speed electric train EKr-1 "Tarpan", which can reach a design speed of up to 200 km/h depending on the modification.

A distinctive feature of the mechanical part of the electric train is the use of a pneumatic suspension system at the second stage of suspension, which enables both stiffness and damping characteristics during oscillations of the car body and bogie [2-4]. These characteristics depend on loading conditions and the force interaction between the wheelset and the track [5]. Additional components include vertical hydraulic dampers, as well as yaw and lateral displacement dampers.

During operation, the electric train interacts forcefully with the railway track. The main excitation factors are vertical and horizontal irregularities. Particular attention should be paid to the lateral deviation of rails in curved track sections, which also acts as an excitation in the dynamic model of the vehicle and can be considered as an irregularity in the horizontal plane.

An increase in the design speed leads to a growth in dynamic performance indicators and, accordingly, to a higher risk of transport incidents. The indicators of dynamic performance of

rolling stock include vertical and lateral dynamic coefficients in the first and second stages of suspension, maximum values of vertical and lateral accelerations of the car body, the ratio of frame force to vertical load, as well as the safety factor against wheel derailment, among others.

In studies of the dynamic behavior of modern railway rolling stock on curved track sections, one of the key parameters is the safety factor against wheel derailment. This indicator comprehensively reflects the conditions of wheel-rail interaction, taking into account the ratio of vertical and lateral forces in the contact zone and their influence on the potential for wheel flange climb onto the rail head. Unlike individual force or kinematic indicators, the safety factor has an integral nature directly related to traffic safety.

The relevance of this indicator increases under conditions of higher operating speeds associated with the introduction of modern rolling stock with improved traction and dynamic characteristics. It is precisely on curved track sections that load redistribution occurs between the wheels of a wheelset, lateral forces and angles of attack increase, thereby raising the risk of loss of stability. Under such conditions, the safety factor provides a quantitative assessment of the safety level and makes it possible to determine permissible speed limits in curved track sections.

Thus, the study of the safety factor against wheel derailment for modern rolling stock, along with the determination of permissible speeds in curved track sections, is a relevant scientific task. It enables comparative analysis of various design solutions, operating conditions, and track parameters, and forms a scientific basis for improving the safety of railway rolling stock operation on curved track sections.

2. Literature review and problem statement

Studies on the dynamic behavior of rolling stock, where the object of investigation is a rail vehicle, are mainly focused on the analysis of force interaction with the track [6]. The main objective of such studies [7, 8] is to identify dynamic phenomena arising during operation, including running stability, dynamic performance in curved track sections, and ride comfort.

In [9], a study was conducted on the ride quality of the high-speed EKr-1 “Tarpan” electric train equipped with a pneumatic suspension system at a speed of 200 km/h. It was shown that the ride quality coefficients of the electric train, both in empty and loaded conditions, are significantly lower than the limit values established in [10]. The study in [9] accounts for the operation of the pressure regulator in the pneumatic spring (air flow depending on the lever rotation angle) as well as the bypass valve. The bypass valve is activated when the pressure difference between the springs of one bogie exceeds a certain threshold value.

In [11], the authors carried out theoretical studies of the dynamic performance of cars of the domestic interregional electric train EKr-1 “Tarpan”. The evaluation of dynamic indicators was performed by simulating the motion of leading and intermediate cars on a straight track section, as well as on curves of medium radius (600 m) and small radius (300 m). In the simulation, the authors used the computer program “DYNRAJL” [12, 13].

For comparison, in [11] the dynamic indicators of the leading car were compared with a reference object-the DS-3 electric locomotive, while for the intermediate car the reference object was the passenger coach model 61-779. It was established that on straight track sections, the main dynamic indicators of both leading and intermediate cars of the electric train do not exceed permissible limits at speeds up to 220 km/h and higher. On curves of medium radius, the values of dynamic indicators also remain within permissible limits – at speeds up to 100 km/h, and on curves of small radius – up to 80 km/h. Moreover, within the considered speed ranges, all obtained dynamic indicators of the leading and intermediate cars of the electric train are better than those of the reference objects. In addition to the main dynamic indicators, wheel wear on the rolling surface and wheel flange wear were also investigated.

In [14], the authors determined permissible speeds for trains with forced tilting of the car body on curved railway track sections. The research methodology was based on the application of a traction-operational model. This model makes it possible to determine the superelevation of the

outer rail in curves and the corresponding length of transition curves, calculate permissible speeds, perform traction calculations, and assess ride comfort [15].

In [16], the authors presented a preliminary assessment of the dynamic performance of passenger cars and selected parameters for the suspension stages of bogie 68-7007 aimed at their improvement and increasing operating speeds. It was found that for passenger cars of models 61-779 and 61-788, there are no issues with vertical dynamics: the values of vertical dynamic coefficients for the car body frame, bogie frame, and ride quality index in the vertical direction are significantly below permissible limits at speeds up to 300 km/h. However, in the study of horizontal dynamics, the value of the horizontal dynamic coefficient of the bogie frame exceeds permissible limits at a speed of 220 km/h. It is emphasized that before determining the parameters of the pneumatic spring of the second (central) suspension stage, it is necessary to address the issue of reducing the horizontal dynamic coefficient of the bogie frame to an acceptable level.

In studies [17, 18], the authors developed a comprehensive approach to modeling rolling stock with pneumatic suspension, based on the coordinated consideration of mechanical and pneumatic processes. Particular attention is paid to investigating the influence of connecting pipeline parameters on system characteristics. The pneumatic model is integrated with a multi-mass model implemented in the SIMPACK environment, which made it possible to carry out a comprehensive analysis of the dynamic behavior of rolling stock.

Within the framework of studies [17, 18], a comparison of two suspension design options (two-point and four-point) was performed, followed by an evaluation of changes in key parameters, including spring deformations, car body tilt angle, and vertical wheel-rail contact forces when negotiating curved track sections. The obtained results demonstrate the effectiveness of the integrated approach to modeling and evaluating the dynamic characteristics of modern rolling stock.

However, the modeling of the pneumatic suspension system does not take into account the variation of the effective area of the air spring during its vertical deformation, nor the vertical stiffness of the rubber-cord bellows, which constitutes a component of the overall vertical stiffness of the air spring. Furthermore, the model assumes a constant total pressure loss coefficient, whereas in reality this coefficient is a variable parameter, as it depends on the airflow velocity through the connecting pipeline.

In [19], a comprehensive three-dimensional model of a high-speed electric train was developed and combined with a thermodynamic description of the pneumatic spring. The analysis of the nonlinear behavior of the spring and its influence on the dynamic performance of rolling stock was carried out using a co-simulation method. The model includes 42 degrees of freedom. The FASTSIM method was used to determine wheel-rail contact forces. Simulation results for motion on a straight track section show that the nonlinear characteristics of the pneumatic spring in the horizontal direction have almost no effect on lateral ride comfort, whereas the vertical characteristics significantly improve comfort. Therefore, the use of a lateral damper between the car body and the bogie is always recommended.

In the study of dynamic behavior on a curved track section, a curve with a radius of 7000 m at a speed of 350 km/h was considered. The obtained results indicate that the nonlinear characteristics of the pneumatic spring have little effect on the vertical wheel-rail force; however, the lateral force in the wheelset and the derailment coefficient increase by approximately 30 %.

In this study, the dynamic characteristics of the pneumatic suspension system were determined solely on the basis of a thermodynamic approach, while the vertical stiffness of the rubber-cord bellows, which has a significant influence on the overall dynamic behavior of the system, was not taken into consideration.

In [20], the influence of active suspension on lateral oscillations of the car body and its horizontal accelerations is investigated. For this purpose, pneumatic actuators installed between the car body and the bogie and integrated with pneumatic springs are proposed. The simulations were carried out for motion on curved track sections. The results showed that the use of active suspension significantly reduces the maximum lateral displacements of the car body compared to

conventional systems.

However, the study did not take into account the heat transfer between the air spring and the surrounding environment, nor the stiffness of the rubber-cord bellows of the air spring.

In [21], the authors studied the effect of the initial setting of the leveling valve lever angle of the pneumatic spring on wheel load imbalance when negotiating small-radius curves. A new procedure for quasi-static curve negotiation analysis is proposed, taking into account a detailed thermodynamic model of the pneumatic suspension, including nonlinear airflow characteristics through the leveling valve and differential pressure valves. A total of 30 curves were considered, with a minimum radius of 160 m and a maximum outer rail superelevation of 105 mm. The speed was set at 30 km/h for curves with a radius greater than 200 m and reduced to 10 km/h for curves below 200 m. As a result, vertical wheel-rail contact forces for the leading axle were obtained for cases without initial lever angle offset and with initial offsets: +1.2° for pneumatic springs 1 and 4 of the car body, and –1.2° for springs 2 and 3.

The mathematical model employed to describe the operation of the pneumatic suspension system does not account for the energy losses arising from the airflow between the air spring and the auxiliary reservoir.

In [22], alternative approaches to the mathematical modeling of pneumatic suspension systems were identified and compared, and their impact on the accuracy of reproducing the dynamics of railway rolling stock was evaluated. It was found that for large-radius curves, the dynamic model of the pneumatic spring produces results close to those of a quasi-static model. The authors emphasize that, in the calculation of wheel–rail contact forces during curve negotiation, modeling the coupling of lateral and roll stiffness in the suspension is more important than accounting for the frequency dependence of vertical stiffness or the variation of lateral/roll stiffness parameters with the load acting on the suspension.

In the considered mathematical model of the pneumatic suspension system, it is assumed that heat transfer between the air spring and the surrounding environment can be neglected, and all thermodynamic processes are treated as adiabatic, which may limit the accuracy of representing real operating conditions.

In [23], the authors performed a dynamic simulation of a high-speed train with a hydropneumatic suspension functioning as a self-steering system. The results showed that the radial arrangement of bogies on curved track sections significantly reduces both wheel-rail system wear and the interaction force of the wheel flange with the rail gauge face.

At the same time, the applied approach represents one of the alternative methods for improving curving performance on railway tracks; however, it does not provide the capability for a comprehensive investigation of the dynamic behavior of high-speed rolling stock equipped with a pneumatic suspension system.

Despite numerous studies devoted to the dynamic interaction between railway vehicles and track, the improvement of mathematical models describing the dynamic behavior of pneumatic suspension systems during vehicle–track interaction, as well as ensuring operational safety and determining permissible speeds of high-speed trains on curved track sections, remains a relevant research challenge. Most existing studies focus primarily on ride comfort assessment; however, there is a need for a more accurate determination of dynamic safety indicators, particularly the derailment safety coefficient (wheel-climb derailment ratio), which characterizes the margin of stability against wheel derailment. Therefore, the task of improving the mathematical model of the dynamic behavior of the high-speed EKr-1 “Tarpan” electric train, taking into account the specific characteristics of its mechanical linkages when negotiating curved track sections, remains a current scientific task. This will allow identification of the patterns of change in the safety factor against wheel derailment and determination of permissible speeds on curved track sections depending on the curve radius.

3. Research objectives and tasks

The aim of this study is to improve the mathematical model of the dynamic interaction between high-speed rolling stock and the track on curved sections. This will make it possible to determine the safety factor against wheel derailment of the high-speed EKr-1 "Tarpan" electric train and establish the maximum permissible speeds when operating on curved track sections.

To achieve this aim, the following tasks need to be accomplished:

– Improve a spatial mathematical model of the dynamic behavior of the high-speed EKr-1 "Tarpan" electric train, taking into account the specific characteristics of its mechanical linkages and the influence of excitations from curved track sections;

– Identify the patterns of variation of the safety factor against wheel derailment depending on the curve radius;

– Determine the maximum permissible speeds of the electric train on curved track sections as a function of the curve radius.

4. Research methodology

4.1. Mathematical model of the dynamic interaction between rolling stock and track on a curved section

The improvement of a comprehensive spatial mathematical model involves several stages:

– Selection of the calculation scheme.

– Formulation of the dynamic equilibrium equations.

– Derivation of geometric relationships between the deformations of the linkages and the coordinates of the calculation scheme.

– Description of the physical relationships between reactions and deformations.

– Analytical representation of external excitations.

The car is represented as a mechanical system consisting of seven rigid bodies connected by elastic and damping elements. The calculation scheme of the leading car of the EKr-1 "Tarpan" electric train is shown in Fig. 1.

Based on the adopted calculation scheme of the car (Fig. 1), its state at any given moment is defined by 26 coordinates. Applying D'Alembert's principle, differential equations for the dynamic system were obtained. Since the safety factor against wheel derailment reflects the ratio of lateral and vertical interaction forces in the wheel–rail system, this work presents the differential equations of the mechanical system components in the horizontal and vertical directions.

For the car body, the differential equations of equilibrium are as follows:

– Bouncing:

$$m_k\ddot{z}_k + \sum_{j=1}^{4} P_j + \sum_{j=1}^{4} P_{v.dampj} + \sum_{j=1}^{4} P_{vj} - m_k g = 0. \tag{1}$$

– Galloping motion:

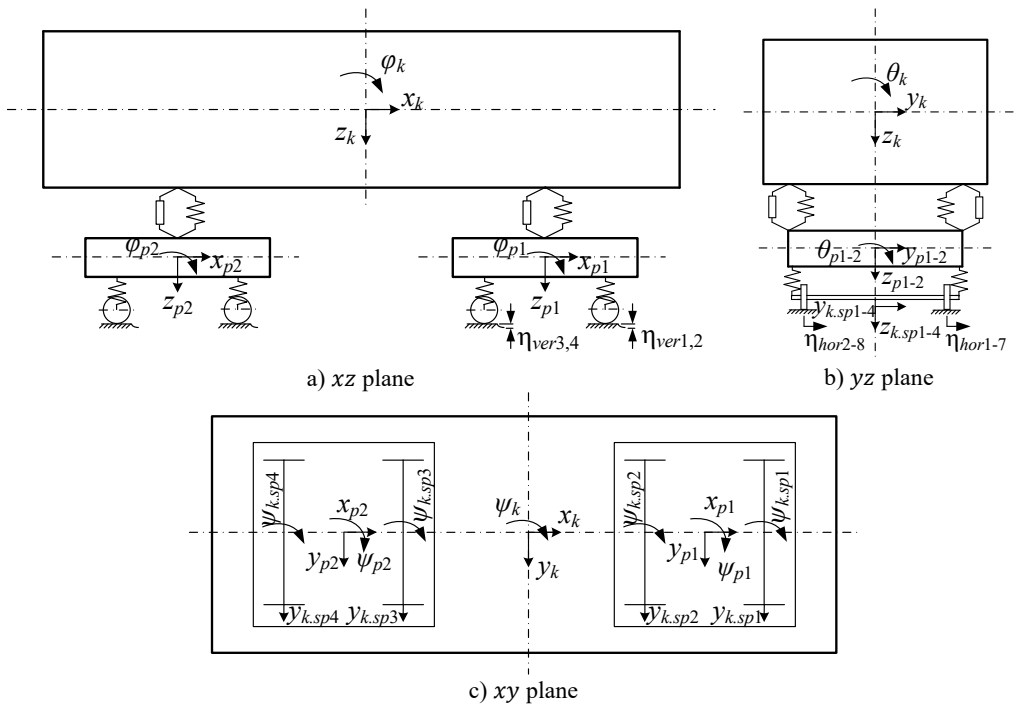
$$J_{yk}\ddot{\varphi}_k + P_1 b + P_2 b - P_3 b - P_4 b + P_{v.damp1} b + P_{v.damp2} b - P_{v.damp3} b - P_{v.damp4} b + P_{v1}(b-l) + P_{v2}(b-l) - P_{v3}(b-l) - P_{v4}(b-l) - \sum_{j=1}^{4} F_j c - \sum_{j=1}^{4} P_{long.vj} c = 0. \tag{2}$$

– Lateral displacement:

$$m_k\ddot{y}_k + \sum_{j=1}^{4} Q_j + \sum_{j=1}^{4} P_{y.vj} + \sum_{j=1}^{4} P_{h.lateralj} = 0. \tag{3}$$

– Lateral sway:

$$J_{xk}\ddot{\theta}_k + P_1 f - P_2 f + P_3 f - P_4 f + P_{v1} f - P_{v2} f + P_{v3} f - P_{v4} f + P_{v.damp1} a - P_{v.damp2} a + P_{v.damp3} a - P_{v.damp4} a - \sum_{j=1}^{4} Q_j\, c - \sum_{j=1}^{4} P_{y.vj}\, c - \sum_{j=1}^{4} \mathrm{P}_{h.lateralj}\, c = 0. \tag{4}$$



a) xz plane b) yz plane

c) xy plane

Fig. 1. Calculation scheme of the EKr-1 "Tarpan" high-speed train car

– Yaw motion:

$$J_{zk}\ddot{\psi}_k + Q_1 b + Q_2 b - Q_3 b - Q_4 b + P_{y.v1} b + P_{y.v2} b - P_{y.v3} b - P_{y.v4} b + P_{h.lateral1} b + P_{h.lateral2} b - P_{h.lateral3} b - P_{h.lateral4} b - F_1 f + F_2 f - F_3 f + F_4 f - P_{long.v1} f + P_{long.v2} f - P_{long.v3} f + P_{long.v4} f = 0, \tag{5}$$

where m_k – mass of the car body; J_{xk}, J_{yk}, J_{zk} – moments of inertia of the car body about the central x, y and z axes; P_j – vertical reactions of the pneumatic springs of the second stage of the suspension; $P_{v.dampj}$ – vertical component of the reaction of the lateral hydraulic dampers in the second stage of the suspension; P_{vj} – vertical reactions of the vertical hydraulic vibration dampers of the second stage suspension; F_j – longitudinal reactions of the pneumatic springs of the second stage suspension; Q_j – lateral reactions of the pneumatic springs of the second stage suspension; $P_{long.vj}$ – longitudinal component of the reaction of the yaw hydraulic dampers in the second stage of the suspension; $P_{y.vj}$ – lateral component of the reaction of the yaw hydraulic dampers in the second stage of the suspension; $P_{h.lateralj}$ – horizontal component of the reaction of the lateral

hydraulic dampers in the second stage of the suspension; f – lateral distance from the geometric center of the car body to the line of action of the vertical reaction of the pneumatic spring; a – lateral distance from the geometric center of the car body to the line of action of the vertical reaction of the lateral hydraulic damper; b – longitudinal distance from the geometric center of the car body to the line of action of the vertical reaction of the pneumatic spring; c – vertical distance from the geometric center of the car body to the top plate of the pneumatic spring.

To determine the vertical reactions of the air springs in high-speed rolling stock, the authors of the paper improved the mathematical model of the pneumatic suspension system, which includes the determination of air pressure in the air spring $P_1(t)$, the auxiliary reservoir $P_2(t)$, the air temperature in the air spring $T_1(t)$ and in the auxiliary reservoir $T_2(t)$, as well as the mass flow rate of air through the connecting pipeline $m(t)$:

$$\dot{P}_1(t) = -\left(1+\frac{R}{C_v}\right)\dot{h}(t)\frac{P_1(t)}{h(t)} - \left(1+\frac{C_p}{C_v}\right)\dot{m}(t)\frac{P_1(t)}{m_1(t)} + \frac{2}{r_1}\frac{R}{C_v}h_T\big(T_s - T_1(t)\big), \tag{6}$$

$$\dot{P}_2(t) = \left(1+\frac{R}{C_v}\right)\dot{m}(t)\frac{P_2(t)}{m_2(t)}, \tag{7}$$

$$\dot{T}_1(t) = -\frac{A_1 P_1(t)\dot{h}(t)}{m_1(t)C_v} - \frac{\dot{m}(t)C_p T_1(t)}{m_1(t)C_v} + \frac{h_T A_s(t)\big(T_s - T_1(t)\big)}{m_1(t)C_v}, \tag{8}$$

$$\dot{T}_2(t) = \frac{\dot{m}(t)C_p T_2(t)}{m_2(t)C_v}, \tag{9}$$

$$\dot{m}(t) = \frac{\left(\frac{\pi}{4}\right)d^2\sqrt{2\rho(t)|P_1(t)-P_2(t)|}}{\sqrt{f\frac{l}{d}+K_S+K_P}}\operatorname{sign}\big(P_1(t)-P_2(t)\big), \tag{10}$$

where P, T – respectively, the pressure and temperature of the working fluid of the pneumatic spring, $m(t)$ – mass airflow rate through the connecting pipeline during the operation of the pneumatic suspension system, R – universal gas constant, A_1 – effective area of the pneumatic spring, $h(t)$ – height of the air spring at a given moment in time, f – Darcy friction factor (along the length of the pipeline); l – length of the connecting pipeline, d – diameter of the connecting pipeline, K_s – loss coefficient for sudden contraction; K_p – loss coefficient for sudden expansion, ρ – density of the working fluid, C_v – specific heat capacity at constant volume, C_p – specific heat capacity at constant pressure, h_T – heat transfer coefficient, T_s – surface temperature of the heat transfer area.

The differential equations of equilibrium for bogie No. 1 are as follows:

– Bouncing:

$$m_{p1}\ddot{z}_{p1} - P_1 - P_2 - P_{v1} - P_{v2} - P_{v.damp1} - P_{v.damp2} + \sum_{i=1}^{4} P_{spi} + \sum_{i=1}^{4} P_{sp.lati} = 0. \tag{11}$$

– Galloping motion:

$$J_{yp1}\ddot{\varphi}_{p1} + P_{v1}l + P_{v2}l + P_{sp1}\varepsilon + P_{sp2}\varepsilon - P_{sp3}\varepsilon - P_{sp4}\varepsilon + P_{sp.lat1}e + P_{sp.lat2}e - P_{sp.lat3}e - P_{sp.lat4}e - F_1 h - F_2 h + P_{sp.x1}w + P_{sp.x2}w + P_{sp.x3}w + P_{sp.x4}w = 0. \tag{12}$$

– Lateral displacement:

$$m_{p1}\ddot{y}_{p1} - Q_1 - Q_2 - P_{y.v1} - P_{y.v2} - P_{h.lateral1} - P_{h.lateral2} + \sum_{j=1}^{4} P_{sp.latj} = 0. \tag{13}$$

– Lateral sway:

$$J_{xp1}\ddot{\theta}_{p1} - P_{v.damp1}a + P_{v.damp2}a - P_1 f + P_2 f - P_{v1}f + P_{v2}f + P_{sp1}f - P_{sp2}f + P_{sp3}f - P_{sp4}f + \ldots P_{damp1}f - P_{damp2}f + P_{damp3}f - P_{damp4}f + P_{h.lateral1}h + P_{h.lateral2}h - \cdots - Q_1 h - Q_2 h + P_{sp.lat1}w + P_{sp.lat2}w + P_{sp.lat3}w + P_{sp.lat4}w = 0. \quad (14)$$

– Yaw motion:

$$J_{zp1}\ddot{\psi}_{p1} + P_{sp.lat1}\varepsilon + P_{sp.lat2}\varepsilon - P_{sp.lat3}\varepsilon - P_{sp.lat4}\varepsilon + F_1 f - F_2 f + P_{long.v1}f - P_{long.v2}f - \ldots P_{sp.x1}f + P_{sp.x2}f - P_{sp.x3}f + P_{sp.x4}f = 0, \quad (15)$$

where m_p – mass of the bogie frame; J_{xp}, J_{yp}, J_{zp} – moments of inertia of the bogie frame about the axes x, y and z; P_{spi} – vertical reactions of the springs of the axlebox stage of the suspension; $P_{sp.xi}$ – longitudinal reactions of the springs of the axlebox stage of the suspension; $P_{sp.latj}$ – lateral reactions of the springs of the axlebox stage of the suspension; $P_{sp.lati}$ – vertical reactions of the hydraulic vibration dampers of the axlebox stage of the suspension; h – vertical distance from the center of gravity of the bogie frame to the pneumatic spring; w – vertical distance from the center of gravity of the bogie frame to the plane of support on the springs of the axlebox suspension; ε – horizontal distance from the center of gravity of the bogie frame to the centers of the springs of the axlebox suspension; e – horizontal distance from the center of gravity of the bogie frame to the line of action of the vertical reaction of the vertical hydraulic dampers of the axlebox suspension.

The differential equations of equilibrium for the first wheelset of bogie No. 1 are as follows.

– Lateral displacement:

$$m_{k.sp1}\ddot{y}_{k.sp1} + F_{y1} + F_{y2} + Q(R_1) - Q(R_2) - P_{sp.lat1} - P_{sp.lat2} = 0. \quad (16)$$

– Yaw motion:

$$J_{z.k.sp1}\ddot{\psi}_{k.sp1} + F_{x1}S - F_{x2}S + P_{sp.x1}S - P_{sp.x2}S = 0, \quad (17)$$

where $m_{k.sp}$ – mass of the wheelset; $J_{z.k.sp}$ – moment of inertia of the wheelset about the axis z; S – distance from the wheel-rail contact point to the center of gravity of the wheelset; F_x – longitudinal reactions at the wheel-rail contact; F_y – lateral reactions at the wheel-rail contact; $Q(R)$ – projections of the normal reaction between the wheel and the rail onto the horizontal y-axis.

The magnitudes of the longitudinal F_x and lateral F_y reactions are described by a nonlinear creep hypothesis:

$$F_x = K\frac{\upsilon_x}{\upsilon}, \quad (18)$$

$$F_y = K\frac{\upsilon_y}{\upsilon}, \quad (19)$$

where K – creep coefficient; υ – speed of the rolling stock; υ_x – longitudinal slip velocity of the wheel on the rail; υ_y – lateral slip velocity of the wheel on the rail.

The longitudinal slip velocities of the wheels of the first wheelset are as follows:

$$\upsilon'_{x1} = \upsilon\frac{\Delta r_1}{r_1} + \dot{\psi}_{k.sp1}S, \quad (20)$$

$$v'_{x2} = v\frac{\Delta r_2}{r_2} - \dot{\psi}_{k.sp1}S. \tag{21}$$

The lateral slip velocities of the wheels are as follows:

$$v'_{y1} = \dot{y}_{k.sp1} - v\psi_{k.sp1}, \tag{22}$$
$$v'_{y2} = \dot{y}_{k.sp1} - v\psi_{k.sp1}, \tag{23}$$

where Δr_j – increment of the wheel radii of the rolling stock wheelsets; r_j – mean radii of the wheels of the rolling stock wheelsets.

The increment of the wheel radii depends on the lateral displacement of the wheelset w_p, the horizontal irregularity η_{hor}, the wheel profile conicity at the contact point with the rail n, and the nominal clearances between the wheel flange and the inner gauge face of the rail head δ_{nom}.

For the wheels of the first wheelset of bogie No. 1, the magnitude of the change in their radii is determined as follows:

$$\Delta r_1 = n_2 y_{k.sp1} - n_2\eta_{hor1r.} + \delta_{nom.1}(n_1 - n_2), \tag{24}$$
$$\Delta r_2 = -n_2 y_{k.sp1} + n_2\eta_{hor1l.} + \delta_{nom.2}(n_1 - n_2), \tag{25}$$

where n_2 – conicity value at the wheel-rail contact point; n_1 – conicity of the wheel tread; $\delta_{nom.j}$ – nominal values of the clearances between the wheel flanges and the inner faces of the rail heads; η_{horj} – values of the horizontal irregularities of the track.

Thus, the improved mathematical model of the pneumatic suspension system of high-speed rolling stock makes it possible to comprehensively account for variations in the effective area of the air spring, the vertical stiffness of the rubber-cord bellows, heat transfer processes with the surrounding environment, mass airflow rate, and energy losses during air exchange between the air spring and the auxiliary reservoir, as well as the geometric parameters of the system components. In contrast to existing approaches, such a model provides a more complete description of the physical processes occurring in the pneumatic suspension system and enables improved accuracy in determining its dynamic characteristics during rolling stock operation.

4.2. Analytical description of rail lateral deviation functions (horizontal irregularities) in curved track sections

The study considers a curve consisting of a straight section, a transition curve, a circular curve, another transition curve, and a straight section (Fig. 2).

The curvature radius in the transition curves can be analytically described by the equation of a radial spiral:

$$R_{cur} = \frac{c_t}{x_{t.s}} = \frac{R_{kkp}\cdot l_{t.s}}{x_{t.s}}, \tag{26}$$

where R_{cur} – radius of curvature; c_t – transition curve parameter; R_{kkp} – radius of the circular curve; $l_{t.s}$ – length of the transition curve; $x_{t.s}$ – abscissa of the track section measured from the beginning of the transition curve.

Adopting an approximate relationship from differential geometry $d^2y/dx^2 = -x_{t.s}/c_t$ and, by integrating it twice, we obtain the equation of the transition curve for section I:

$$y = -\frac{{x_{t.s}}^3}{6c_{1t}} + A_1 x_{t.s} + B_1. \tag{27}$$

At the entry to the circular curve (section II), the equation of the track lateral deviation takes the form:

$$y = -y_{0\ kk} + \sqrt{R_{kkp}{}^2 - (x_{t.s} - x_{0\ kk})^2}, \tag{28}$$

where $x_{0\ kk}$, $y_{0\ kk}$ – coordinates of the center of the circular curve.

At the exit from the circular curve into the transition curve (Section 3), the equation of the track lateral deviation takes the form:

$$y = -\frac{(x_{max} - x_{t.s})^3}{6c_{2t}} + A_2 x_{t.s} + B_2. \tag{29}$$

In Eq. (27-29), the unknown coefficients are determined by the conditions of equality of the derivatives at the junction points of the parabolas and the circle, M_1 and M_2, as well as by the equality of ordinates at the same points.

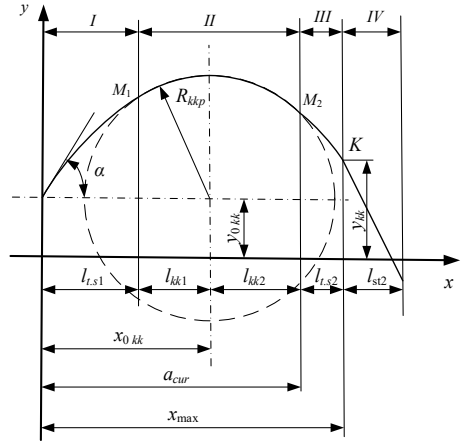


Fig. 2. Scheme of the connection of the curve sections

To avoid jumps in the derivative of the resulting function when entering the curved section, it is necessary to switch to a global coordinate system by shifting the origin of the curve along the Oy axis by a distance B_1 and rotating it relative to the Ox axis by an angle α.

This rotation is performed using the formula:

$$\eta_{hor.cur} = x_{t.s} \sin\alpha - y \cos\alpha, \tag{30}$$

where $\eta_{hor.cur}$ – lateral deviation function of the track in the "rotated" coordinate system; $x_{t.s}$, y – coordinates of the curved track contour in the local coordinate system.

He track gauge widening in the transition and circular curves was modeled by varying the structural clearance between the wheel flange and the rail head. This clearance changes linearly from δ_{nj} to δ_{max}. In the circular curve, it remains constant at δ_{max}, and then decreases back to δ_{nj}, i.e., to the value equal to the clearance on the straight track section.

Thus, having the mathematical model of the dynamic behavior of the high-speed rolling stock, we now consider how the safety factor against wheel derailment is evaluated.

4.3. Methodology for determining the safety factor against wheel derailment

The stability of a wheelset against derailment is checked for the most critical cases, where a

large lateral force from the rolling wheel on the rail coincides with a small vertical load on the same wheel. When these forces act simultaneously over a period of time, the flange of the rolling wheel may climb onto the rail head, potentially causing the car to derail (Fig. 3).

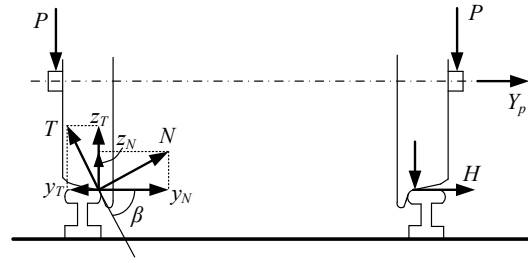


Fig. 3. Forces acting during the interaction of the wheelset with the rail: β – angle of inclination of the straight portion of the wheel flange profile relative to the track plane; Y_p – frame (lateral) force [24]; N – reaction force of the rail on the wheel flange; T – friction force between the flange and the rail head

Based on mathematical transformations, the safety factor against wheel derailment can be determined using the formula:

$$\lambda = \frac{P}{Z_T + Z_N} = \frac{P}{Y'} \cdot \frac{\mathrm{tg}\beta - \mu}{\mu \mathrm{tg}\beta + 1}. \tag{31}$$

In this case, the stability condition is expressed as:

$$\lambda \geq [\lambda], \tag{32}$$

where $[\lambda]$ – permissible value of the wheel safety factor against derailment [25].

5. Research results

5.1. Determination of the patterns of change in the frame (lateral) force of the EKr-1 "Tarpan" train car with respect to the curve radius of the track section

The initial data for modeling the dynamic behavior of the EKr-1 "Tarpan" high-speed electric train consisted of technical and operational parameters of the rolling stock, as well as characteristics of its suspension systems and wheel–rail interaction: m_k = 69048 kg, J_{xk} = 91592 kg·m^2, J_{yk} = 2409050 kg·m^2, J_{zk} = 2414020 kg·m^2, f = 1,018 m, a = 0,258 m, b = 6.2 m, c = 1.675 m, J_{xp} = 5653 kg·m^2, J_{yp} = 10546 kg·m^2, J_{zp} = 15557 kg·m^2, h = 0.1 m, w = 0.371 m, ε = 1.4 m, e = 1.67 m, $J_{z.k.sp.}$ = 634.35 kg·m^2, S = 0,8 m.

In the study, the curve radius of the track section varied between 300 and 4000 m, while the maximum cant of the outer rail and track widening were taken as 150 mm and 10 mm, respectively. The nominal clearance between the wheel flange and the side face of the rail head was set at 9 mm.

Based on multi-variant iterative calculations of the dynamic behavior of the EKr-1 "Tarpan" train in the Matlab environment, graphs of the frame (lateral) force variation at the maximum permissible speed were obtained, determined by the condition that the frame force does not exceed 30 % of the static vertical load of the wheelset on the track (Fig. 4).

Based on the obtained results, it was established that an increase in train speed leads to a rise in the frame (lateral) force at a constant curve radius. For R_{kkp} = 300 m, as the speed increases from 60 to 100 km/h, the maximum frame force rises from 37.8 to 61.7 kN, corresponding to a 63.2 % increase. For R_{kkp} = 500 m, the frame force increases from 32.35 to 52.3 kN, a 61.7 %

increase, and for R_{kkp} = 800 m, it rises from 25.1 to 47.23 kN, an 88.2 % increase. A similar trend is observed for curve radii in the range R_{kkp} = 1000-4000 m and speeds of 100-160 km/h.

The dependencies of the frame force on the curve radius at different speeds are shown in Fig. 5.

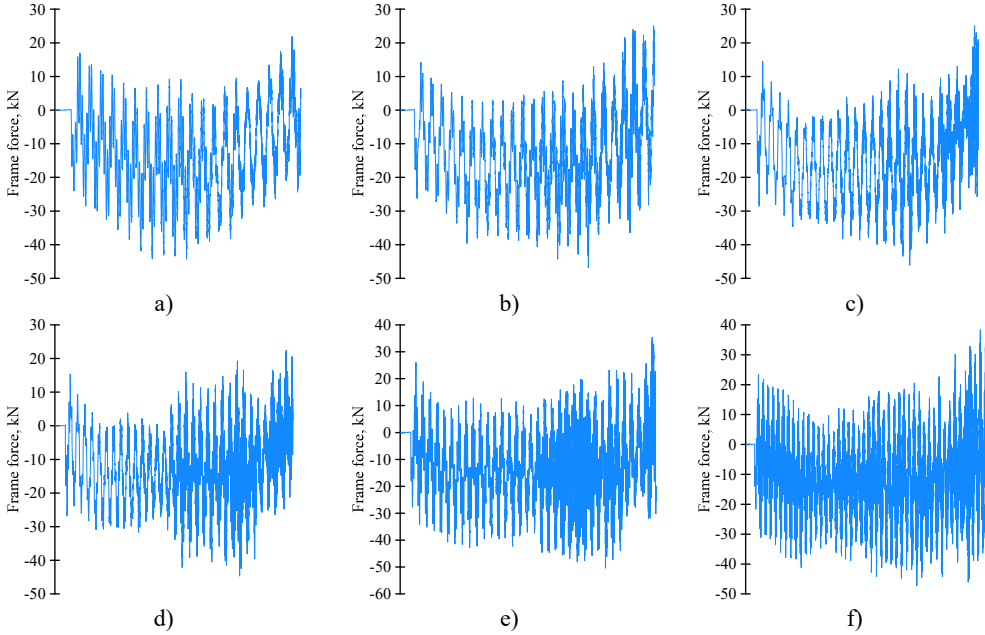


Fig. 4. Variation of the frame (lateral) force of the EKr-1 "Tarpan" train car at the maximum permissible speed on a curved track section with a radius of: a) R_{kkp} = 300 m; b) R_{kkp} = 400 m; c) R_{kkp} = 500 m; d) R_{kkp} = 600 m; e) R_{kkp} = 700 m; f) R_{kkp} = 800 m

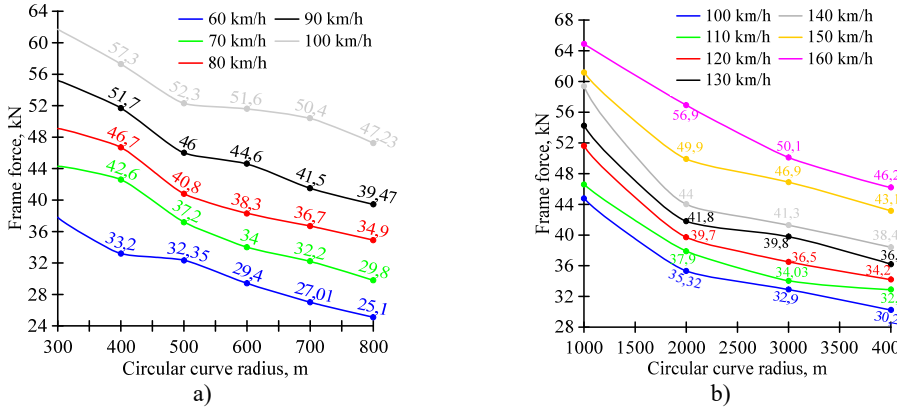


Fig. 5. Dependence of the frame (lateral) force on the track curve radius for the following speed ranges: a) 60-100 km/h; b) 100-160 km/h

It was established that increasing the curve radius of the track section leads to a decrease in the frame (lateral) force, allowing the rolling stock to operate at higher speeds. The maximum reduction in the frame force, expressed as a percentage, occurs at a speed of 60 km/h when the curve radius increases from R_{kkp} = 300 m to R_{kkp} = 800 m, and at a speed of 140 km/h for radii from R_{kkp} = 1000 m to R_{kkp} = 4000 m, amounting to 50.6 % and 54.7 %, respectively.

The obtained frame force values allow proceeding to the determination of the safety factor against wheel derailment and the establishment of the speed ranges within which the safe operation

ISSN PRINT 2351-5279, ISSN ONLINE 2424-4627

of the rolling stock is ensured.

5.2. Investigation of the safety factor against wheel derailment and determination of maximum permissible speeds on curved track sections

Based on the obtained frame force values, an investigation of the safety factor against wheel derailment was carried out for different speeds and curve radii of the railway track (Tables 1-2). A speed is considered permissible if the safety factor against wheel derailment is greater than 1.4.

Table 1. Safety factor against wheel derailment of the EKr-1 "Tarpan" train car on curves with radii of R_{kkp} = 300-800 m

R_{kkp}. m	v. km/h				
	60	70	80	90	100
300	1.63	1.51	1.43	1.35	1.28
400	1.73	1.54	1.47	1.39	1.33
500	1.75	1.64	1.57	1.48	1.39
600	1.83	1.71	1.62	1.51	1.40
700	1.9	1.76	1.67	1.56	1.42
800	1.96	1.82	1.69	1.60	1.46

Table 2. Safety factor against wheel derailment of the EKr-1 "Tarpan" train car on curves with radii of R_{kkp} = 1000-4000 m

R_{kkp}. m	v. km/h						
	100	110	120	130	140	150	160
1000	1.50	1.47	1.40	1.37	1.30	1.28	1.25
2000	1.68	1.63	1.59	1.55	1.52	1.42	1.33
3000	1.74	1.67	1.63	1.59	1.56	1.47	1.42
4000	1.81	1.73	1.67	1.64	1.61	1.53	1.48

Based on the obtained results, it was established that an increase in speed leads to a decrease in the safety factor against wheel derailment at a constant curve radius. For R_{kkp} = 300 m, as the speed increases from 60 to 100 km/h, the safety factor decreases from 1.63 to 1.28; for R_{kkp} = 400 m – from 1.73 to 1.33; for R_{kkp} = 500 m – from 1.75 to 1.39; for R_{kkp} = 600 m – from 1.83 to 1.4; for R_{kkp} = 700 m – from 1.9 to 1.42; and for R_{kkp} = 800 m – from 1.96 to 1.46.

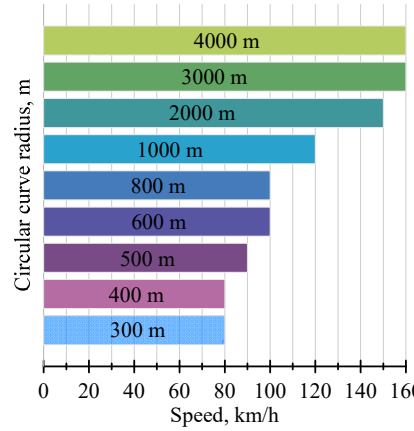


Fig. 6. Permissible speeds of the EKr-1 "Tarpan" train when moving along a curved track section

To assess the adequacy of the numerical results, they were compared with published experimental data reported in [26]. That study presents the derailment safety coefficients for a straight track section and a curved track section with a radius of 600 m at an operating speed of

100 km/h. Based on the data reported in [26], the ratio of the derailment safety coefficients for the straight and curved track sections is 1.23. According to the results presented in Tables 1-2, the corresponding ratio obtained from the numerical simulation at an operating speed of 100 km/h is 1.29. The relative difference between these values does not exceed 5 %, indicating good agreement between the numerical results and the published experimental data.

By applying the requirement that the safety factor against wheel derailment must be at least 1.4, the permissible speeds of the EKr-1 "Tarpan" train on curved track sections were determined, and corresponding recommendations were provided (Fig. 6).

The determined permissible speeds ensure the operation of the high-speed rolling stock with maximum throughput while maintaining the required level of operational safety.

6. Discussion of the obtained results

A spatial mathematical model of the dynamic behavior of rolling stock interacting with the railway track has been developed, enabling the analysis of horizontal and vertical forces in the wheel-rail system. This model provides a foundation for further determination of operational safety indicators, specifically the safety factor against wheel derailment and the permissible speeds on curved track sections.

A key feature of the study was the effect of curved track sections on the dynamic characteristics of modern rolling stock with a pneumatic spring suspension system. The curve was modeled as a horizontal irregularity described by the track lateral deviation function. Additionally, modeling included the cant of the outer rail and track widening in the curve.

The results of the mathematical modeling of the dynamic behavior of the rolling stock on curved track sections revealed patterns in the variation of the frame (lateral) force and the safety factor against wheel derailment depending on the curve radius and speed. It was shown that increasing the curve radius reduces the frame force and increases the safety factor, which positively allows the rolling stock to operate at higher speeds.

The permissible speeds based on the safety factor against wheel derailment were determined as follows: R_{kkp} = 300 m-80 km/h, R_{kkp} = 500 m-90 km/h, R_{kkp} = 800 m-100 km/h, R_{kkp} = 1000 m-120 km/h, R_{kkp} = 2000 m-150 km/h, R_{kkp} = 3000÷4000 m-160 km/h.

Analysis of the dynamic behavior of the EKr-1 "Tarpan" high-speed train shows that on curved track sections, the maximum permissible speed is 160 km/h, which limits the full realization of high-speed operation.

At the same time, the mathematical approach proposed in this study is not limited exclusively to the investigation of the EKr-1 "Tarpan" electric train. The structure of the spatial mathematical model can be adapted to investigate the dynamic behavior of other types of railway rolling stock by taking into account their structural, mass-inertial, and dynamic characteristics, as well as the parameters and characteristics of individual mechanical constraints and suspension components.

7. Conclusions

Based on the analysis of literature sources and the mathematical modeling of the dynamic behavior of rolling stock on curved track sections, the following conclusions were drawn:

A spatial mathematical model of the dynamic behavior of the high-speed EKr-1 "Tarpan" train was developed, taking into account the features of its pneumatic spring suspension system when moving along a curved track section. The calculation scheme of the car assumes that the positions of its structural elements at any given moment are defined using 26 generalized coordinates. The curve is included in the mathematical model through an analytical description of the track lateral deviation functions (horizontal irregularities) in curved sections of the track.

Patterns of change in the frame (lateral) force and the safety factor against wheel derailment depending on the curve radius at different train speeds were established. It was shown that increasing the curve radius leads to a decrease in the frame force and an increase in the safety

factor, allowing the rolling stock to operate at higher speeds. The maximum reduction in the frame force, expressed as a percentage, occurs at a speed of 60 km/h with an increase in curve radius from 300 m to 800 m, and at a speed of 140 km/h for radii from 1000 m to 4000 m, amounting to 50.6 % and 54.7 %, respectively.

Based on the obtained safety factor values against wheel derailment, permissible speeds were determined. It was established that for a curve radius of R_{kkp} = 300 m, the permissible speed is 80 km/h; for R_{kkp} = 500 m-90 km/h; for R_{kkp} = 800 m-100 km/h; for R_{kkp} = 1000 m-120 km/h; for R_{kkp} = 2000 m-150 km/h; and for R_{kkp} = 3000÷4000 m-160 km/h.

It was shown that on curved track sections, the maximum permissible speed is 160 km/h, which limits the full realization of high-speed operation.

Acknowledgements

The authors have not disclosed any funding.

Data availability

The datasets generated during and/or analyzed during the current study are available from the corresponding author on reasonable request.

Author contributions

Kuzyshyn Andrii: conceptualization, project administration, validation. Kovalchuk Vitalii: methodology, resources. Pentsak Andriy: investigation; visualization.

Conflict of interest

The authors declare that they have no conflict of interest.

References

[1] A. Kuzyshyn et al., "Research of safety indicators of diesel train movement with two-stage spring suspension," *MATEC Web of Conferences*, Vol. 234, p. 05003, Nov. 2018, https://doi.org/10.1051/matecconf/201823405003

[2] A. Kuzyshyn, V. Kovalchuk, M. Sysyn, and Y. Sobolevska, "Influence of the geometric parameters of the connecting pipeline on the stiffness and damping of the pneumatic spring suspension at high-speed rolling stock," *Vehicle System Dynamics*, Vol. 64, No. 1, pp. 155–176, Jan. 2026, https://doi.org/10.1080/00423114.2024.2425022

[3] A. Kuzyshyn, V. Kovalchuk, Y. Royko, I. Kravets, and Y. Sobolevska, "Determination of dynamic characteristics and features of operation of pneumatic springs of high-speed railway rolling stock, while changing the pressure gauge in the spring," *Acta Polytechnica Hungarica*, Vol. 22, No. 4, pp. 173–192, Jan. 2025, https://doi.org/10.12700/aph.22.4.2025.4.11

[4] A. Kuzyshyn, V. Kovalchuk, Y. Sobolevska, Y. Royko, and I. Kravets, "Determining the effect of additional tank volume and air pressure in the spring on the dynamic indicators of a pneumatic system of spring suspension in high-speed railroad rolling stock," *Eastern-European Journal of Enterprise Technologies*, Vol. 3, No. 7 (129), pp. 47–62, Jun. 2024, https://doi.org/10.15587/1729-4061.2024.304051

[5] A. Kuzyshyn, V. Kovalchuk, and Y. Royko, "Effects of movement direction through a switch on accelerations and natural frequencies of a pneumatic suspension of high-speed rolling stock," *Communications – Scientific Letters of the University of Žilina*, Vol. 27, No. 1, pp. 53–64, 2025, https://doi.org/10.26552/com.c.2025.007

[6] A. Kuzyshyn, A. Batig, S. Kostritsa, J. Sobolevska, S. Dovhaniuk, and V. Dzhus, "Study of the dynamic behavior of rolling stock using a computer experiment," *IOP Conference Series: Materials Science and Engineering*, Vol. 985, No. 1, p. 012002, Nov. 2020, https://doi.org/10.1088/1757-899x/985/1/012002

[7] N. Wilson et al., "Assessment of safety against derailment using simulations and vehicle acceptance tests: a worldwide comparison of state-of-the-art assessment methods," *Vehicle System Dynamics*, Vol. 49, No. 7, pp. 1113–1157, Jun. 2011, https://doi.org/10.1080/00423114.2011.586706

[8] B. Suarez, J. M. Mera, M. L. Martinez, and J. A. Chover, "Assessment of the influence of the elastic properties of rail vehicle suspensions on safety, ride quality and track fatigue," *Vehicle System Dynamics*, Vol. 51, No. 2, pp. 280–300, Sep. 2012, https://doi.org/10.1080/00423114.2012.725852

[9] O. Safronov, P. Khozia, Y. Vodiannykov, and S. Stoletov, "Ride quality of the high-speed electric train EKr-1 "Tarpan" with air-spring suspension at the speed of 200 km/h," (in Ukrainian), *Collection of Scientific Works of the State University of Infrastructure and Technologies Series "Transport Systems and Technologies"*, Vol. 33, No. 1, pp. 189–201, 2019, https://doi.org/10.32703/2617-9040-2019-33-1-16

[10] "Passenger Cars. Ride Quality. Methods of Determination," (in Ukrainian), Ministry of Industrial Policy of Ukraine, SOU MPP 45.060-204:2007, 2007.

[11] A. N. Pshynko, S. V. Myamlin, and M. V. Kramarenko, "Theoretical studies of the dynamic performance of cars of the domestic interregional dual-system electric train EKr-1 "Tarpan"," (in Ukrainian), *Vagonnyy Park*, Vol. 3-4, pp. 120–121, 2017.

[12] S. V. Myamlin, "Computer program "Dynamics of Rail Vehicles" (DYNRAIL)," (in Ukrainian), Mar. 2003.

[13] S. V. Myamlin, "Evaluation of dynamic performance indicators of the head and intermediate cars of the interregional dual-system electric train manufactured by PJSC Kryukiv Railway Car Building Works," (in Ukrainian), *Railway Transport of Ukraine*, Vol. 5, pp. 48–56, 2012.

[14] M. B. Kurgan, D. M. Kurgan, and V. I. Kharlan, "Determination of permissible train speeds with forced car body tilting on curved track sections," (in Ukrainian), *Bulletin of the Dnipropetrovsk National University of Railway Transport Named After Academician V. Lazaryan*, Vol. 12, pp. 47–52, 2006.

[15] M. B. Kurhan, I. P. Korzhenevych, and V. V. Arsonov, "Organization of high-speed traffic with the use of rolling stock with a forced tilt body cars," (in Ukrainian), *Science and Transport Progress*, Vol. 11, No. 11, pp. 50–59, 2006, https://doi.org/10.15802/stp2006/18619

[16] S. V. Myamlin and V. V. Zhizhko, "The search for the optimal parameters of the spring suspension trucks passenger cars," (in Ukrainian), *Science and Transport Progress*, Vol. 30, No. 30, pp. 173–182, 2009, https://doi.org/10.15802/stp2009/14625

[17] N. Docquier, P. Fisette, and H. Jeanmart, "Model-based evaluation of railway pneumatic suspensions," *Vehicle System Dynamics*, Vol. 46, No. sup1, pp. 481–493, 2008, https://doi.org/10.1080/00423110801993110

[18] N. Docquier, "Multiphysics modelling of multibody systems application to railway pneumatic suspensions," *Université Catholique De Louvain*, Vol. 48, No. 12, pp. 1439–1460, 2010, https://doi.org/10.1080/00423110903509335

[19] Z. Qi, F. Li, and D. Yu, "A three-dimensional coupled dynamics model of the air spring of a high-speed electric multiple unit train," *Proceedings of the Institution of Mechanical Engineers, Part F: Journal of Rail and Rapid Transit*, Vol. 231, No. 1, pp. 3–18, Aug. 2016, https://doi.org/10.1177/0954409715620534

[20] A. C. Mellado, C. Casanueva, J. Vinolas, and J. G. Giménez, "A lateral active suspension for conventional railway bogies," *Vehicle System Dynamics*, Vol. 47, No. 1, pp. 1–14, Aug. 2008, https://doi.org/10.1080/00423110701877512

[21] T. Tanaka and H. Sugiyama, "Prediction of railway wheel load unbalance induced by air suspension leveling valves using quasi-steady curve negotiation analysis procedure," *Proceedings of the Institution of Mechanical Engineers, Part K: Journal of Multi-body Dynamics*, Vol. 234, No. 1, pp. 19–37, 2019, https://doi.org/10.1177/1464419319867179

[22] A. Facchinetti, L. Mazzola, S. Alfi, and S. Bruni, "Mathematical modelling of the secondary airspring suspension in railway vehicles and its effect on safety and ride comfort," *Vehicle System Dynamics*, Vol. 48, No. sup1, pp. 429–449, Nov. 2010, https://doi.org/10.1080/00423114.2010.486036

[23] R. Luo and C. Liu, "Dynamics simulation of the high-speed train using interconnected hydro-pneumatic suspension as a self-steering system," *Vehicle System Dynamics*, Vol. 60, No. 6, pp. 2055–2074, Jun. 2022, https://doi.org/10.1080/00423114.2021.1892156

[24] V. Kovalchuk, A. Kuzyshyn, S. Kostritsya, Y. Sobolevska, A. Batig, and S. Dovganyuk, "Improving a methodology of theoretical determination of the frame and directing forces in modern diesel trains," *Eastern-European Journal of Enterprise Technologies*, Vol. 6, No. 7 (96), pp. 19–26, 2018, https://doi.org/10.15587/1729-4061.2018.149838

[25] "Standards for Permissible Speeds of Rolling Stock on 1520 mm Gauge Railway Tracks of the State Administration of Railway Transport of Ukraine: TsP-0235," (in Ukrainian), Ukrzaliznytsia, Kyiv, 2011.

[26] A. N. Pshynko, S. V. Myamlin, M. V. Kramarenko, and V. N. Duzyk, "Results of the operation of dual-system interregional electric trains on the railways of Ukraine," *Lokomotyv-Inform*, Vol. 3–4, No. 129–130, pp. 39–44, 2017.



Kuzyshyn Andrii Yaroslavovych, Ph.D., Associate Professor, Deputy Director of the Institute of Mechanical Engineering and Transport, Lviv Polytechnic National University (Lviv, Ukraine). Research interests: interaction between rolling stock and track, theoretical and experimental studies of rail vehicle dynamics, modeling of the dynamic behavior of rail vehicles, forensic examination of railway transport investigations.



Kovalchuk Vitalii Volodymyrovych, Doctor of Technical Sciences, Professor, Professor of the Department of Railway Transport, Lviv Polytechnic National University (Lviv, Ukraine). Research interests: static and dynamic testing of railway and road transport stuctures, monitoring and assessment of their technical condition, methods and models for assessing the load-bearing capacity of transport structures under various loads.



Pentsak Andriy Yaroslavovych, Ph.D., Associate Professor, Department of Building Production Lviv Polytechnic National University (Lviv.Ukraine). Research interests: stress-strain analysis of a sleeve connection for reinforcing bars in reinforced concrete beams, capacity of reinforced concrete beams restored using injection methods